

Comparison of the Numerical Model with Experimental Data for a Beam-Loss Monitor Based on an Optical Fiber

Yu. I. Maltseva^{a,*} and K. V. Astrelina^a

^a*Budker Institute of Nuclear Physics, Siberian Branch, Russian Academy of Sciences, Novosibirsk, 630090 Russia*

**e-mail: yuliya.maltseva@gmail.com*

Received October 17, 2019; revised December 16, 2019; accepted February 28, 2020

Abstract—The principle of operation of a distributed beam-loss monitor based on Cherenkov radiation in an optical fiber is considered. This device makes it possible to obtain a real-time distribution of losses across the entire accelerator. A numerical model of the monitor describing its spatial resolution is developed for various scenarios of the beam losses. Ways to improve the monitor are considered. It is shown that the simulation results are in good agreement with the experimental data obtained on the e^-e^+ injection complex at the Budker Institute of Nuclear Physics.

DOI: 10.1134/S1547477120040305

INTRODUCTION

A distributed beam-loss monitor on the basis of Vavilov–Cherenkov radiation in optical fibers was proposed for diagnostics of beam losses on the e^-e^+ Injection Complex at the Budker Institute of Nuclear Physics (BINP) [1].

This monitor has a number of advantages. The use of optical fiber with a length of about 40 m saves space near the accelerator vacuum chamber and reduces the number of electronic devices for signal processing. Owing to the insensitivity to the magnetic field, the optical fiber can be mounted inside the magnetic elements, thereby increasing the accuracy of measurements. Due to the nature of Cherenkov radiation, the monitor does not have any noise associated with gamma or synchrotron radiation. Using a photomultiplier with a gain of $\sim 10^6$ as a photodetector, the monitor is capable of recording beam losses at a level of 1% (0.1 nC).

The disadvantages of the monitor are the inaccuracy of localizing the place of the beam loss and the difficulty of absolutely calibrating the losses due to the attenuation and dispersion of the light pulse.

To study the factors that determine the spatial resolution of the beam-loss monitor and ways to improve it, a numerical model was created using the FLUKA program [2]. The spatial resolution of the monitor is determined by the dispersion of light in the fiber and the time characteristics of the photodetector and the analog to digital converter (ADC), and it also depends on which end of the fiber the light pulses are recorded. To confirm the monitor parameters obtained by numerical simulation, a prototype of the

monitor was created on the electron section of the Injection Complex.

1. DISPERSION OF LIGHT IN OPTICAL FIBER

There are two main types of dispersion in fiber: modal and chromatic. When a pulse is transmitted over a multimode optical fiber with a length L and a stepped profile of the refractive index, the contribution of each of the dispersions to the pulse broadening can be estimated as [3]:

$$t_{\text{mod}}/L \approx NA^2/(2cn), \quad t_{\text{chr}}/L \approx \Delta n(\lambda)/c,$$

where NA is the numerical aperture, c is the speed of light in vacuum, n is the refractive index of the fiber core, and $\Delta n(\lambda)$ determines the spectral width of radiation.

For plastic fiber ($NA = 0.47$, $n = 1.49$), the contribution of modal and chromatic dispersion to the duration of the output signal in the range of UV and visible light wavelengths (300–700 nm) is $t_{\text{mod}}/L \approx 0.25$ ns/m, $t_{\text{chr}}/L \approx 0.08$ ns/m, respectively. Thus, in a plastic fiber for the visible wavelength range, the broadening of the light signal due to the modal dispersion is a factor of three higher than the chromatic dispersion.

To determine the contribution of dispersion to the pulse broadening depending on the fiber length, the beam losses were measured in the end of a 300-MeV linear electron accelerator. The beam was lost at the location of the optical fiber using a magnetic corrector.

For the test, a plastic multimode fiber with a stepped refractive index profile (HFBR-RUS500Z, Broadcom) was selected. The fiber parameters were as

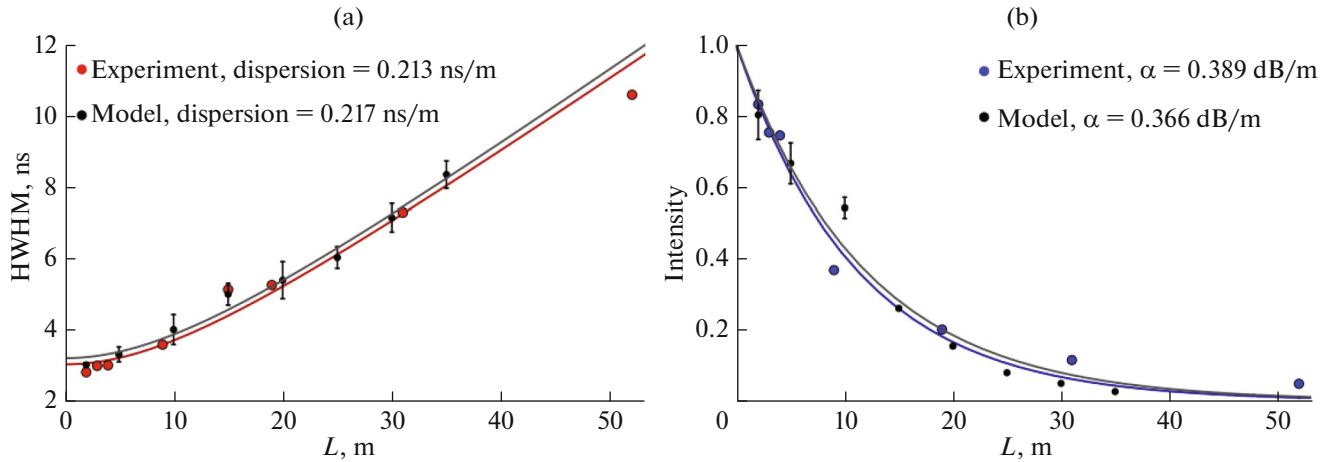


Fig. 1. (a) FWHM of the signals from the photomultiplier at different lengths of plastic multimode fiber: (red) measured and (black) model; (b) photomultiplier signal at different lengths of plastic multimode fiber: (red) measured and (black) model.

follows: core diameter 1 mm; $NA = 0.47$, $n = 1.49$, and attenuation coefficient 0.22 dB/m at 660 nm. As a photodetector, we selected a microchannel plate-based photomultiplier (MCP-PMT) (JSC “Katod”, Novosibirsk) with a maximum of photocathode spectral sensitivity range corresponding to the maximum of the Cherenkov radiation spectrum (300–900 nm); the front rise time of the MCP-PMT is 0.5 ns and the duration (FWHM) of the anode current pulse is at least 1.5 ns. The ADC selected for the experiment had a bandwidth of 200 MHz and a sampling rate of 2 G sample/s.

Figure 1a shows experimental data and numerical simulations of the FWHM of the output signal at different lengths of the fiber segment; the measured contribution of the MCP-PMT of approximately 3.3 ns to the resulting pulse broadening was added to the numerical simulation of the light dispersion in the optical fiber. The dispersion of light in the fiber, obtained taking into account experimental errors, is approximately 0.213 ns/m. This value indicates the predominance of modal dispersion in plastic fiber with a stepped profile of the refractive index. The experimental data are in good agreement with the results of numerical modeling and analytical calculations. For a fiber longer than 20 m, the contributions due to the finite time resolution of MCP-PMT and electronics are insignificant compared to the contribution of dispersion.

2. LIGHT ATTENUATION IN THE FIBER

In addition to dispersion, light propagating through the fiber is subjected to attenuation. The power loss can be calculated using the following formula:

$$P_{\text{output}} = P_{\text{input}} 10^{-\alpha L/10},$$

where P_{output} , P_{input} is the output and input power, respectively; α is the attenuation coefficient (dB/m); and L is the fiber length.

Figure 1b shows experimental data and a numerical simulation of the intensity of the output light signal from the fiber, normalized to the input signal, at different lengths of the fiber segment. The results of numerical simulation are in good agreement with the experimental data. After passing through a 15-m-long fiber, the light signal is reduced by 70% due to losses in the fiber. An approximation of the experimental data results in a damping coefficient of 0.389 dB/m. This value is slightly higher than in the manufacturer’s specification, since the Cherenkov radiation spectrum is shifted to the UV region, where the light attenuation is stronger.

3. SPATIAL RESOLUTION OF THE MONITOR

To determine the location of the beam loss along the accelerator structure, it is necessary to recalculate the time of arrival of the signal from the monitor to the longitudinal coordinate. Due to the wide angular distribution of charged particles, the Cherenkov radiation propagates along the fiber both in the direction of the primary beam (direction 1) and in the opposite direction (direction 2). Therefore, the light signal can be registered at both ends of the fiber. Since the speed of the beam is greater than the speed of light propagation in the fiber, the sampling step along the coordinate when the signal is recorded at the fiber end can be expressed as:

$$s_1 \approx \frac{c}{f(n-1)}, \quad (1)$$

$$s_2 \approx \frac{c}{f(n+1)}, \quad (2)$$

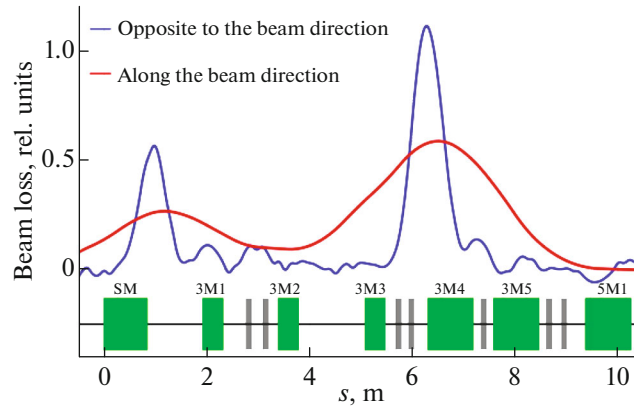


Fig. 2. Losses of the electron beam in the injection channel from the storage ring obtained from two ends of the optical fiber. The first loss occurs after the septum magnet and the second is due to the beam discharge with the use of the 3M3 correction magnet.

where s_1, s_2 is the sampling step along the coordinate when the pulse is recorded at the fiber end located along and against the beam propagation direction, respectively; f is the ADC sampling rate.

Thus, for a plastic fiber ($n = 1.49$), the spatial resolution of the monitor when the signal is recorded in the direction opposite to the beam propagation direction is five times better than the resolution when the signal is recorded in the direction of beam propagation. According to the numerical model, the intensity of the signal in the former case will be an order of magnitude lower than in the latter case.

Figure 2 shows the distribution of electron-beam losses in the output channel of the 500 MeV output storage ring obtained at two ends of the optical fiber. In both cases, the monitor registers two main beam losses: at the point where the beam is injected from the storage ring (after the septum magnet SM) and where the 3M3 magnetic dipole correction is used. The FWHMs and intensity ratios of these signals are given in Table 1.

Based on the values given in Table 1, it can be concluded that the signal propagating oppositely to the beam can improve the spatial resolution of the beam-loss monitor by 4–5 times when compared to the sig-

nal propagating in the beam direction. At the same MCP-PMT gain coefficient, the signal intensity will be much lower. Both of these conclusions are in good agreement with the results of analytical calculations and numerical modeling.

Considering the results on the distortion of the monitor output signal depending on the fiber length (Fig. 1) and Eqs. (1) and (2) for calculating the sampling increment of spatial resolution, it can be concluded that, to achieve a spatial resolution of the monitor no worse than 1 m, which is required for the fiber-optic monitor for the Injection Complex at BINP SB RAS, the optimal fiber length should be 20 m. The attenuation in the optical fiber of such a length will result in the loss of up to 80% of radiation.

CONCLUSIONS

In this paper, we studied the dependences of the spatial resolution of the beam-loss monitor and the intensity of the output signal depending on the length of the optical fiber for the case of a multimode plastic fiber with a stepped profile of the refractive index. The estimates are in good agreement with experimental data.

Table 1. Results of signal processing shown in Fig. 3

Place of loss	Direction of signal propagation	Distance to MCP-PMT, m	Spatial resolution, m	Ratio of signal 1 to signal 2
SM	1	19	3.1	9.3
	2	16	0.6	
3M3	1	14.5	3.0	10.9
	2	20.5	0.7	

The best spatial resolution of the monitor is achieved when the light signal is recorded at the fiber end opposite to the beam propagation direction. The photomultiplier based on multichannel plate is characterized by a high time resolution and is recommended as a detector of the light signal for the beam-loss monitor. The ADC for the monitor should have a bandwidth of at least 200 MHz. In order to achieve a spatial resolution of at least 1 m, which is required for the fiber-optic beam-loss monitor for the Injection Complex at the Budker Institute of Nuclear Physics, it is necessary to use fibers with a length of at least 20 m, as well as fast electronics.

REFERENCES

1. E. Nebot del Busto et al., in *Proceedings of the IBIC 2014, 4th International Beam Instrumentation Conference, Melbourne, Australia, September 13–17, 2015*, p. 580.
2. X.-M. Marechal, Y. Asano, and T. Itoga, *Nucl. Instrum. Methods Phys. Res., Sect. A* **673**, 32–45 (2012).
3. Yu. Maltseva et al., in *Proceedings of the 26th Russian Particle Accelerator Conference RuPAC2018, Protvino, Russia, October 1–5, 2018*, p. 39.
4. Yu. I. Maltseva et al., *Phys. Usp.* **58**, 516–519 (2015).
5. Yu. Maltseva and V. G. Prisekin, in *Proceedings of the 26th Russian Particle Accelerator Conference RuPAC2018, Protvino, Russia, October 1–5, 2018*, p. 486.
6. G. Battistoni et al., *Ann. Nucl. Energy*, 10–18 (2015).
7. J. M. Senior, *Optical Fiber Communications Principles and Practice*, 3rd ed. (Pearson Education, 2009).

Translated by V. Alekseev